ORIGINAL ARTICLE

An experimental study on the in-plane behavior of interlocking blocks with different interconnection mechanisms

Vahid Baneshi · Seyed Mehdi Dehghan · Reza Hassanli

Abstract The utilization of interlocking systems in masonry structures provides numerous advantages, such as decreased construction time, improved construction quality, and enhanced structural integrity. Despite these advantages, the behavior of interlocking blocks is still not fully understood due to the variations in the construction methods and the geometry of these blocks around the world. Considering the limited capacity, as well as the inherent brittle behavior of walls built with interlocking blocks under extreme loads, it is crucial to employ supplementary techniques that enhance structural behavior and increase ductility through various connecting mechanisms. This experimental study aims to investigate the effectiveness of adhesive paste as an alternative to mortar, and its combination with grout and steel rebar to improve the structural performance of these walls. The proposed interlocking system is designed with middle and side holes to facilitate incorporating the connecting elements. For this purpose, compression, diagonal shear, and in-plane shear behaviors of specimens made up of blocks interconnected with adhesive paste, grout and steel rebar were tested and the results including failure mode, strength, and force–displacement response were discussed. Under compressive loading, the use of adhesive paste between the blocks effectively increased the strength of the masonry prism. In the diagonal and direct shear tests, where the interlocking keys are directly engaged, the presence of paste and grout was found to have a positive influence on the capacity. The incorporation of grout, steel rebar, and adhesive paste substantially improved the ductility as well as the strength in different loading conditions.

Keywords Adhesive paste · Interlocking block · In-plane behavior · Force–displacement behavior · Failure mechanism

V. Baneshi · S. M. Dehghan (✉)
Department of Civil and Environmental Engineering, Shiraz University of Technology, P.O. Box 313, Shiraz 71555, Iran
e-mail: smdehghan@sutech.ac.ir

V. Baneshi
e-mail: v.baneshi@sutech.ac.ir

R. Hassanli
University of South Australia, Mawson Lakes, SA, Australia
e-mail: reza.hassanli@unisa.edu.au

1 Introduction

Although conventional masonry structures have shown poor structural performance especially against severe loads such as earthquakes and explosions [1], they are still the common structural system for low-rise buildings around the world. Interlocking blocks and mortarless systems are some of the new methods to solve the problems in traditional masonry structures [2]. Interlocking systems significantly increase

efficiency [3, 4], reduce the need for skilled masons, increase wall resistance [5, 6], improve integrity, reduce the construction time [7], and significantly increase the quality of construction [8–10]. Various types of interlocking blocks have been constructed in recent decades [11–18]. These blocks have been built based on the materials and technologies of different countries and they show different behaviors during loading [19–21].

Most previous studies focused on the properties of the dry-stocked blocks including the in-plane and out-of-plane compressive and shear behavior of walls as well as the seismic performance of masonry structures constructed with mortarless interlocking blocks [22–25]. Due to the relative movements of the interlocking blocks, the walls constructed with these types of blocks have weaknesses against in-plane and out-of-plane loads such as earthquakes and eccentric gravity loads. To address this shortcoming and to improve the behavior and integrity of interlocking masonry systems, different techniques could be employed such as grouting, reinforcement with steel bars, applying post-tensioning force [26–32], and using coating or a combination of these methods. However, few studies have been conducted on reinforcing these types of blocks and investigating their in-plane and out-of-plane behavior.

Kasinikota et al. investigated the effects of grouting, and reinforcement layout on the out-of-plane flexural behavior of interlocking hollow block walls [33]. It was concluded that grout and steel reinforcements increased the flexural capacity of the walls and prevented the sudden failure of the walls.

Kohail et al. performed cyclic in-plane tests on the walls constructed with interlocking blocks where post-tensioning, grouting, and reinforcing bars were also incorporated [34]. It was found that the post-tensioned walls with grout improved displacement, energy dissipation, and effective stiffness.

Ma et al. investigated the effect of injecting grout into the vertical holes in interlocking walls and reported that it was successful in removing the gap between the blocks during construction and hence increased the stability of the wall [35].

Zahra et al. performed in-plane and out-of-plane shear tests on reinforced mortarless concrete interlocking blocks. They explored the failure pattern and the load–displacement relationship of the samples with different values of reinforcement ratios and shear span ratios [36]. The results showed that the change in the reinforcement and shear span ratio had a significant effect on the shear strength and behavior of the samples.

Various studies have been conducted on interlocking blocks to investigate different aspects of their mechanical behavior. In many of these studies, testing has been carried out on the mortarless system with post-tension loading. However, the application of post-tension is time-consuming and necessitates the access to special tools and skilled workers, making it impractical for construction practice. Moreover, few researches have investigated the use of conventional mortar in interlocking blocks.

Masonry adhesive, also known as adhesive paste, is an alternative to mortar that simplifies the process of building masonry structures. It offers several advantages over traditional mortar for masonry construction, including strong adhesion, speedy construction, ease of use, reduced surface unevenness, decreased material consumption and waste, as well as elimination of the need for skilled labor. Additionally, due to its lower thickness and greater adhesion, it improves the stability, capacity and integrity of mortarless masonry walls.

In this study, the effectiveness of employing adhesive paste solely and in combination with grout and reinforcing bars in providing higher strength, as well as a degree of ductility, to the proposed interlocking system is examined. The interlocking block with middle and side holes has a distinctive shape that facilitates the incorporation of connecting elements such as grout and steel rebar. To gain a comprehensive understanding of the in-plane behavior of this system with additional connecting mechanisms, a series of tests were conducted. Compression, in-plane shear, and diagonal shear tests were performed to investigate the blocks with various connecting conditions. The obtained results, including load-deformation response, mechanical properties, and failure modes, were compared and discussed.

2 Research significance and objectives

Conventional masonry units typically have flat surfaces, relying on mortar and friction between the surfaces to provide integrity and resistance against loading. To enhance their performance, interlocking

blocks can be used as a substitute. The mechanical performance of interlocking blocks is influenced by their geometric shape and interconnection mechanism. Furthermore, it is possible to improve the behavior of these blocks through various methods, such as using adhesive paste, grout, and rebar. These techniques have led to the construction of masonry walls that are not only cost-effective but also sustainable in nature.

The study focuses on evaluating the in-plane behavior of the proposed interlocking block using adhesive paste as a replacement for mortar. Additionally, it examines the influence of combining adhesive paste with grout and rebar in the interlocking system. The results obtained from this research can provide fundamental information for the design and numerical analysis of masonry walls. Furthermore, by comparing different interconnection conditions, a comprehensive understanding of the design of the walls and their in-plane behavior can be achieved.

3 Geometry and manufacturing of the proposed interlocking block

3.1 Geometric characteristics of the blocks

In the current research, an innovative type of interlocking block was designed with the dimensions of $150 \times 150 \times 300$ mm and the geometric characteristics shown in Fig. 1a. The shape and geometry of the locks of the proposed block were selected based on a previous study of the authors [37] considering the influence of the interlocking configuration on different aspects of the in-plane and out-of-plane behaviors.

In this block, there is one circular hole in the middle and two half-cycle cut-outs on the sides with a diameter of 40 mm. This shape blocks was designed to facilitate construction and at the same time to provide suitable options to interconnect the blocks using adhesive paste, grouting, and steel rebar. The blocks were composed of two symmetrical trapezoidal keys on the top surface and cut-outs on the bottom surface (see Fig. 1a) which were designed to lock in the horizontal relative in-plane movement and in the out-of-plane relative rotation of the blocks.

For ease of wall construction and also to provide a space in between the blocks for adhesive paste application the proposed block had a gap between the upper

and lower keys so that the cut-outs were slightly larger than the keys as shown in Fig. 1b. The gap between the interlocking block keys has also been considered in previous studies [38]. As shown in Fig. 1c, in addition to standard blocks, half blocks, top blocks, and bottom blocks were constructed to build different types of specimens.

3.2 Manufacturing of blocks

The interlocking blocks of the present study were cast in steel and polyethylene molds cut and assembled with an accuracy of 0.2 mm (Fig. 2). The molds were made in two pieces for the easy removal of the samples and preventing damage to the blocks (Fig. 2). The molds were removed one day after cast, before curing of the blocks in water for 28 days.

3.3 Locking mechanism of the designed block

The locking mechanism of the proposed block relies on the physical engagement of the embedded top and bottom keys, as well as the interaction of the side and middle holes of the blocks when they are filled with grout and reinforced. Figure 3 illustrates the locking mechanism between the blocks under in-plane and out-of-plane loads. The keys in the block provide in-plane shear load transfer in the direction of the red arrow. Past research [39] has shown that the keys also play an effective role in supporting out-of-plane bending about the vertical axis through the torsion-shear action [40] along the axis of the block keys (as denoted by the green arrow for the key due to its extension across the block's width and blue arrow for the grouted holes). Furthermore, the blocks have two semicircular holes on the sides and one circular hole in the middle, each with a diameter of 40 mm. When filled with reinforcing elements like grout and rebar, these holes enhance resistance against out-of-plane shear transfer (blue arrow) and out-of-plane bending (green arrow), while ensuring structural integrity between adjacent blocks.

Fig. 1 The proposed inter-
locking block (dimensions
are in mm): **a**. Geometry
of the block, **b**. The gap
between the block keys, **c**.
Types of interlocking block

(a)

(b)

(c)
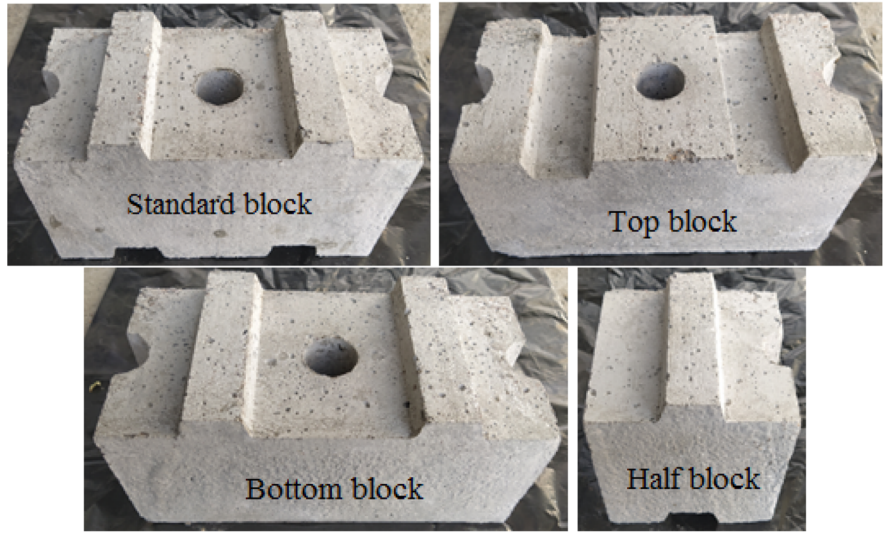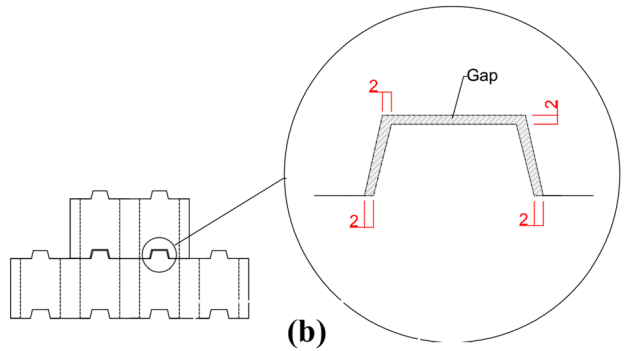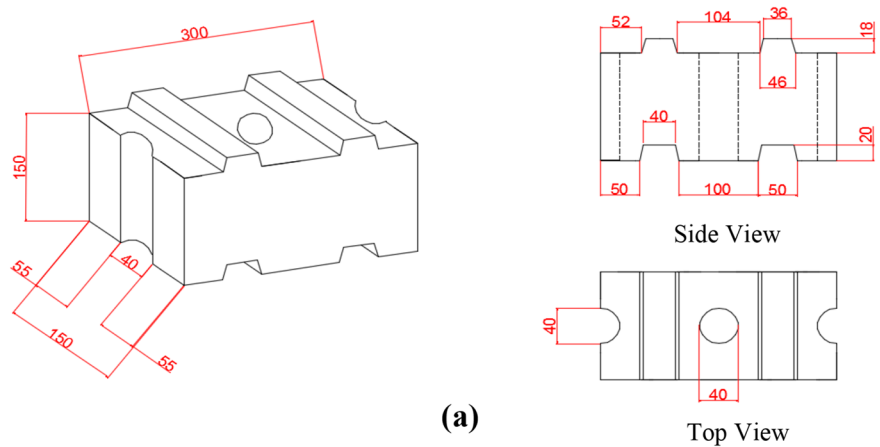
4 Material properties and fabrication of specimens

4.1 Interlocking blocks

To manufacture the interlocking blocks, a combination of mineral sand with maximum grain size of 4.0 mm and Portland cement type II with a

cement-to-sand ratio of 1:3, and water-to-cement ratio of 0.65 was used.

The strength and workability properties of the materials were measured and are presented in Table 1. The properties of the block materials were selected based on the experience of past studies [41, 42].

4.2 Adhesive paste

In the construction of the block prisms, a silica-based cement paste was used as the adhesive material. After the powder was mixed with water with a water-to-powder ratio of 0.3, it became a smooth uniform paste. A thin layer of adhesive paste was used to connect the blocks together. The properties of the used adhesive are presented in Table 1. These properties were determined using the same test methods as the block materials. In addition, the maximum grain size and wet density of this paste were 0.4 mm and 1600 kg/m^3, respectively. Figure 4a shows how to apply paste evenly between the block layers in the constructed prisms using a cloth funnel. By sliding the blocks on top of each other, the paste was spread almost uniformly across the width of the blocks forming a thin layer of paste. On average, approximately 3.6 kg of paste (equivalent to the paste layer thickness of 1~2 mm per course) was utilized per square meter of the wall. This amount is significantly lower compared to the mortar consumption of roughly 25 kg/m^2 used for

Fig. 2 Interlocking block molds

Fig. 3 The locking mechanism of the proposed block

Out-of-plane bending about vertical axis

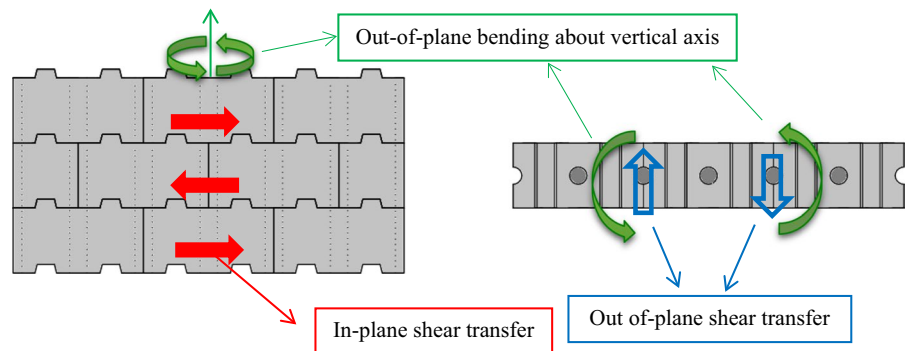In-plane shear transfer

Out of-plane shear transfer

Table 1 The strength and workability properties of the materials

Material	Compressive strength (MPa) ASTM C109 [43]	Flexural strength (MPa) ASTM C348 [44]	Flow—standard	W/C or W/P
Block	26.7 (4.8)	5.2 (19)	112 (%)—ASTM C1437 [45]	0.65
Adhesive Paste	8.7 (3.2)	3.6 (21)	42 (%)—ASTM C1437 [45]	0.3
Grout	24.3 (4.1)	4.1 (17)	20 (sec)—ASTM C1107 [46]	0.25

Value in parentheses represent coefficient of variation in percentage
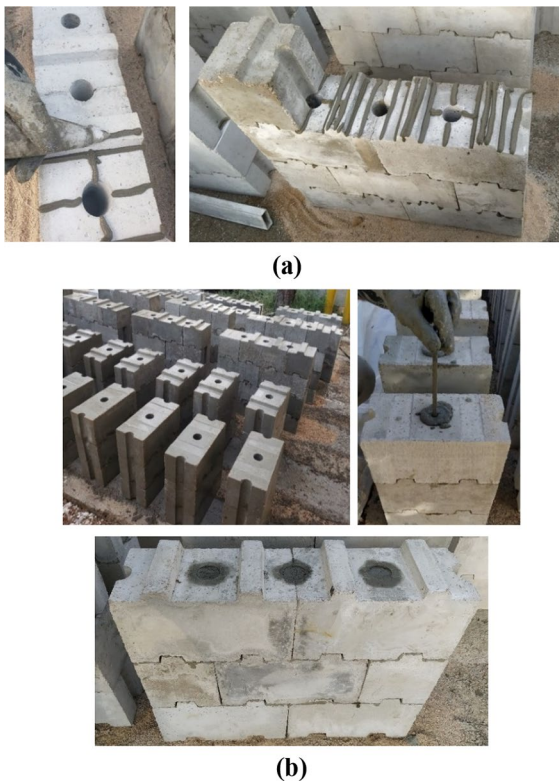
(a)

(b)

Fig. 4 Fabrication of the specimens: **a**. Applying the adhesive paste, **b**. Construction of block prisms and panels

masonry units with the same dimensions and bed joints of 10 mm thickness.

4.3 Grout and rebar

The grout was tested based on ASTM C1107 and its properties are presented in Table 1. Due to the small size of holes in the block a high slump grout was used.

The reinforcing steel rebar had a diameter of 8 mm. It exhibited a yield stress of 240 MPa, an ultimate stress of 370 MPa, a modulus of elasticity of 200,000 MPa, and an elongation at break of 21%.

4.4 Fabrication of specimens

Specimens with different block interconnection conditions were fabricated including (a) adhesive paste, (b) adhesive paste and grout, (c) adhesive paste, grout, and rebar, (d) grout, and (e) grout and rebar. These interconnection conditions are denoted as A,

AG, AGR, G and GR, respectively hereafter. For the compression test, the prisms were also investigated in the dry-stack mortarless (M) condition besides the five mentioned conditions. The average friction coefficient between the dry-stack blocks in M mode is 0.7 [24].

For the pasted specimens, after applying silica-based adhesive mainly on the shear key projection of the lower block (see Fig. 4a), the block of the upper course was assembled. By sliding and slightly pushing the blocks, the paste filled the gap between the blocks (as shown in Fig. 1b) and proper position of the block was set. It's important to note that the paste was only used for the horizontal joints of the blocks. For the reinforced specimens, a rebar with an appropriate length was inserted into the fresh grout and the excessive material was removed. It should be noted that for all test conditions, the prisms were cured under sack and plastic for 28 days after construction before being tested.

In this study, a total of 150 standard blocks, 60 half blocks, 15 top blocks, and 15 bottom blocks were produced by means of ten molds (Fig. 2). For the tests, 45 samples were assembled. Figure 4b shows the constructed samples as well as the method of injecting grout and installing rebar in the assembled block prisms.

5 Experimental program

In this research, the in-plane behavior of masonry including compressive, diagonal shear, and in-plane shear response was quantitatively and qualitatively investigated.

5.1 Compression test

The prisms were constructed and tested in accordance with ASTM C1314 [47]. The samples were constructed by placing three blocks on top of each other as the standard block in the middle, the top block at the top, and the bottom block at the bottom with the dimensions of $150 \times 300 \times 450$ mm (width, length, and height, respectively). Figure 5a shows the details of the compression test. The displacement of the samples was measured by a 0.001 mm precision displacement gauge with a center-to-center distance of 350 mm as shown in Fig. 5a. The

Fig. 5 Setup of tests: **a**. Compression test, **b**. Diagonal shear test, **c**. In-plane shear test
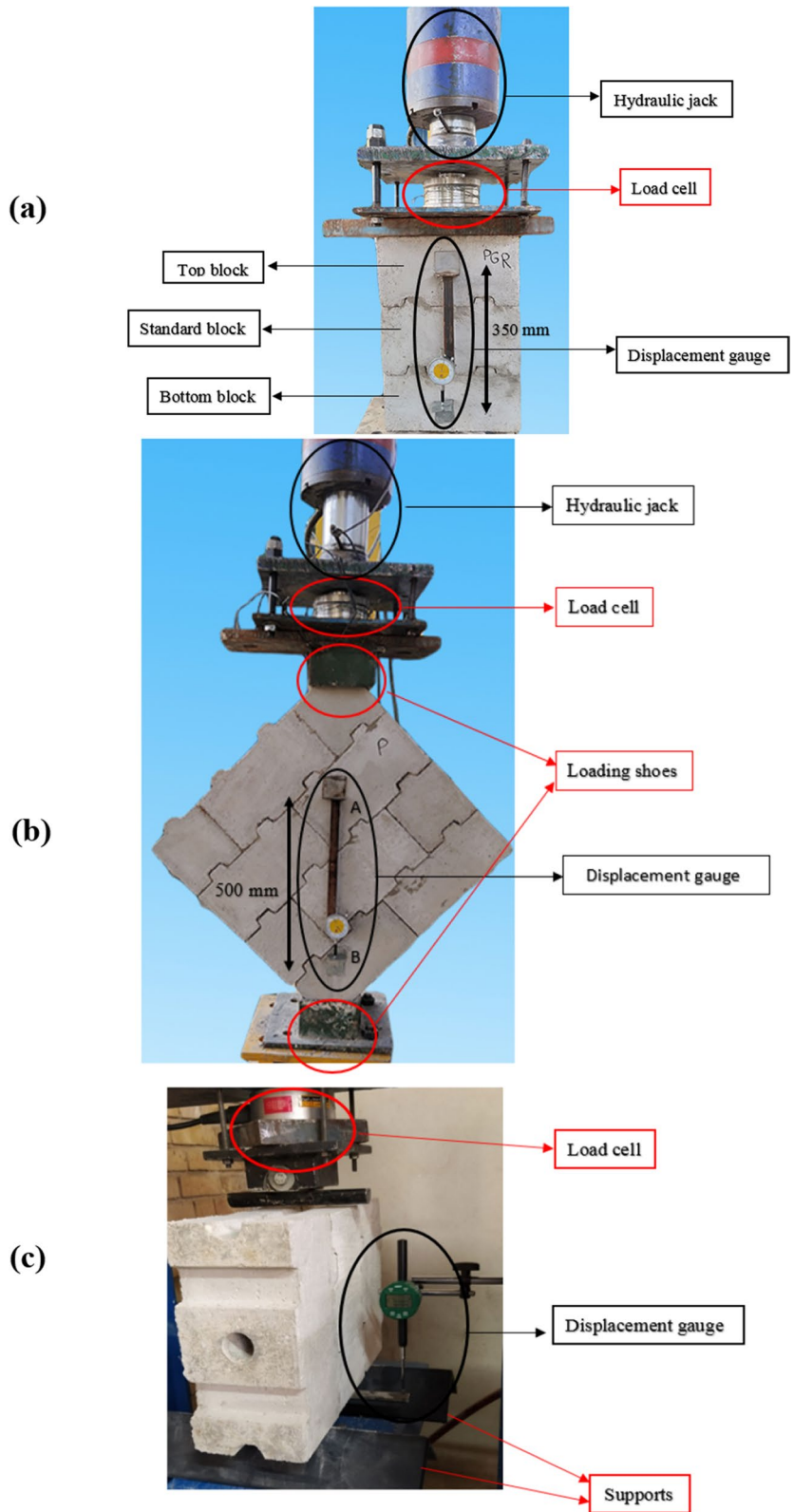
stress of the samples was also calculated by dividing the load by the net surface of the prisms. The reported results were the average values obtained from three block prisms made in each condition.

5.2 Diagonal shear test

The diagonal shear (tension) strength was determined according to the test procedure provided by ASTM E519 [48]. The shear test panels had a thickess × length × width of 150 × 600 × 600 mm, as presented in Fig. 5b. As shown, the panels were loaded diagonally at the top and bottom by two steel loading shoes prescribed by ASTM E519.

As shown in Fig. 5b, the relative displacement between points A and B which had a center-to-center distance of 500 mm on the loading diameter of the panel, was measured using 0.001 precision displacement gauges. These gauges were used on both side of the panel and the average results are presented here. The reported results represent the average values obtained from three block panels manufactured under each specific condition.

5.3 In-plane shear test

To determine the in-plane shear capacity of the samples, triplet test method was adopted as per the previous studies [49]. As shown in Fig. 5c. three-block prisms were placed vertically on two steel supports.

The distance between the supports was 200 mm and the load was applied to the center of the middle block. A digital displacement gauge was used to measure the relative movement of the middle block with respect to the adjacent blocks (see Fig. 5c). The reported values represent the average results obtained from three samples prepared for each interconnecting case.

6 Results and discussion

The force–displacement characteristics, type of cracking, and failure modes of the samples are presented and reviewed hereafter.

6.1 Compression test

6.1.1 Compressive strength

The results of the average compressive strength of the prisms constructed with different interconnection conditions are presented in Table 2.

The block prisms in the AGR and M modes exhibited the highest (16.0 MPa) and lowest (11.6 MPa) compressive strengths among different connection conditions, respectively. A comparison of the compressive strength of mode A and M shows that adding paste (A) and filling the empty space between the blocks with paste improves the continuity and uniform transfer of force between the blocks. As a result, the compressive strength of mode A is higher than mode M. Furthermore, the addition of adhesive, grout, and rebar to the block prism (AGR) increased the compressive strength by 38%. Through a comparison of the compressive strengths between the M and A modes, A and AG modes, and AG and AGR modes, it can be concluded that using adhesive in connecting the block prisms resulted in a 12% increase in compressive strength. Moreover, reinforcing the masonry prisms with grout led to a 15% increase in compressive strength. Lastly, incorporating rebar into the grout and adhesive further enhanced the compressive strength by 7%. Due to the relatively small diameter of the rebar used in prisms compared to the dimensions of the prisms, there was a slight variation in the compressive strength between the AG and AGR modes. As a result, by adding grout to the connections of the block prisms, the highest increase in compressive strength among different connection and reinforcement conditions was achieved. Assessing the effect of grout on the compressive strength

Table 2 Properties of masonry prisms under compression test

Prism connection type	Compressive strength (MPa)	Initial tangent modulus (MPa)	Strain at peak stress
M	11.6 (9.6)	6659 (13)	0.0050 (14)
A	13.0 (13)	6672 (15)	0.0053 (16)
AG	14.9 (10)	7043 (14)	0.0059 (15)
AGR	16.0 (11)	6958 (16)	0.0062 (17)
G	13.6 (8.9)	6747 (11)	0.0054 (15)

Value in parentheses represent coefficient of variation in percentage

(A versus AG and M versus G) showed that grouting almost added the same amount of strength to mortarless and pasted prisms.

6.1.2 Stress–strain characteristics

The stress–strain characteristics are presented in Table 2 and Fig. 6, respectively. In general, the elastic moduli of block prisms have little difference with each other compared to the compressive strength. Comparing the initial moduli of the weakest (M) and strongest connection modes (AGR) in the blocks (4.5% difference), shows that adding adhesive, grout, and rebar to the masonry prisms has a greater effect on their compression strength (38%) than their initial stiffness. As plotted in Fig. 6, it can be observed that the initial slope of all modes remains similar until cracking occurs, which takes place at around 0.001 strain.

According to Fig. 6 and the strain values at the maximum stress in Table 2, it can be concluded that the AGR mode has the highest and the M mode has the lowest relative ductility among the different modes of block prisms. This can be due to the presence of rebar in the grout and its buckling (Fig. 7a).

6.1.3 Crack and type of failure

According to ASTM C1314 [47], the failure type of the A, AG, AGR, and G prisms was more of the conical and semi-conical type. The failures and cracks occurred on the surface of the blocks so that the cracks spread along the length of the samples and adhesive layers (Fig. 7b). In addition, some failures in the grout and buckling of rebar were also observed in the AG and AGR prisms. Based on the graph in Fig. 6, it is evident that in almost all modes, the initial cracks formed on the surface of the blocks within the strain range of 0.001. Subsequently, as the compressive load increased, the length and depth of the cracks escalated in all prisms, reaching a strain of approximately 0.0032. Ultimately, under continued loading, the prisms experienced final failure (Fig. 7).

In M and G cases, due to the empty space between the keys and the resulting stress concentration in the contact area of the block, in addition to conical failure, shear failure also occurred (Fig. 7c). This failure has also been observed in previous studies [38]. Furthermore, the width and depth of the cracks in the G and M modes were greater than in the other modes due to the absence of paste and the discontinuity between the blocks.

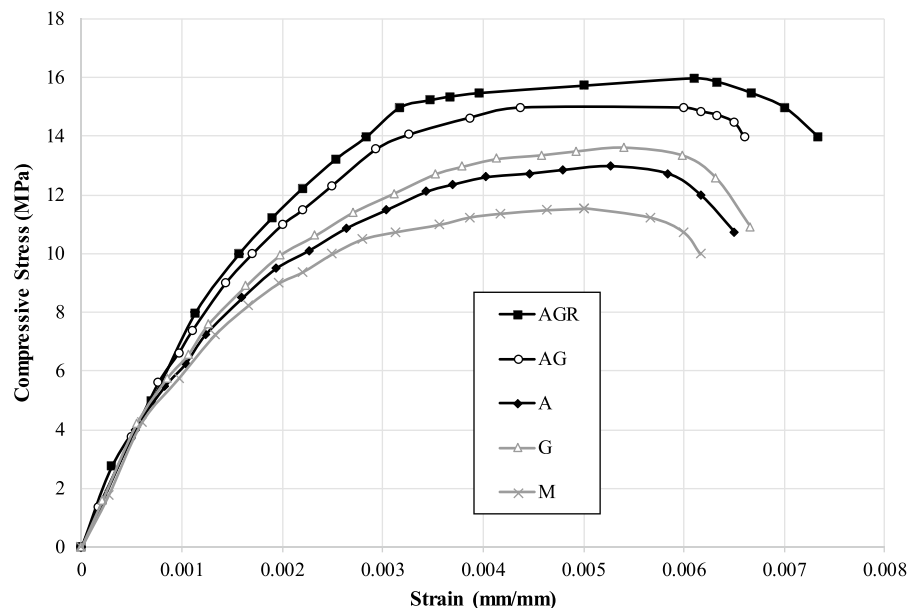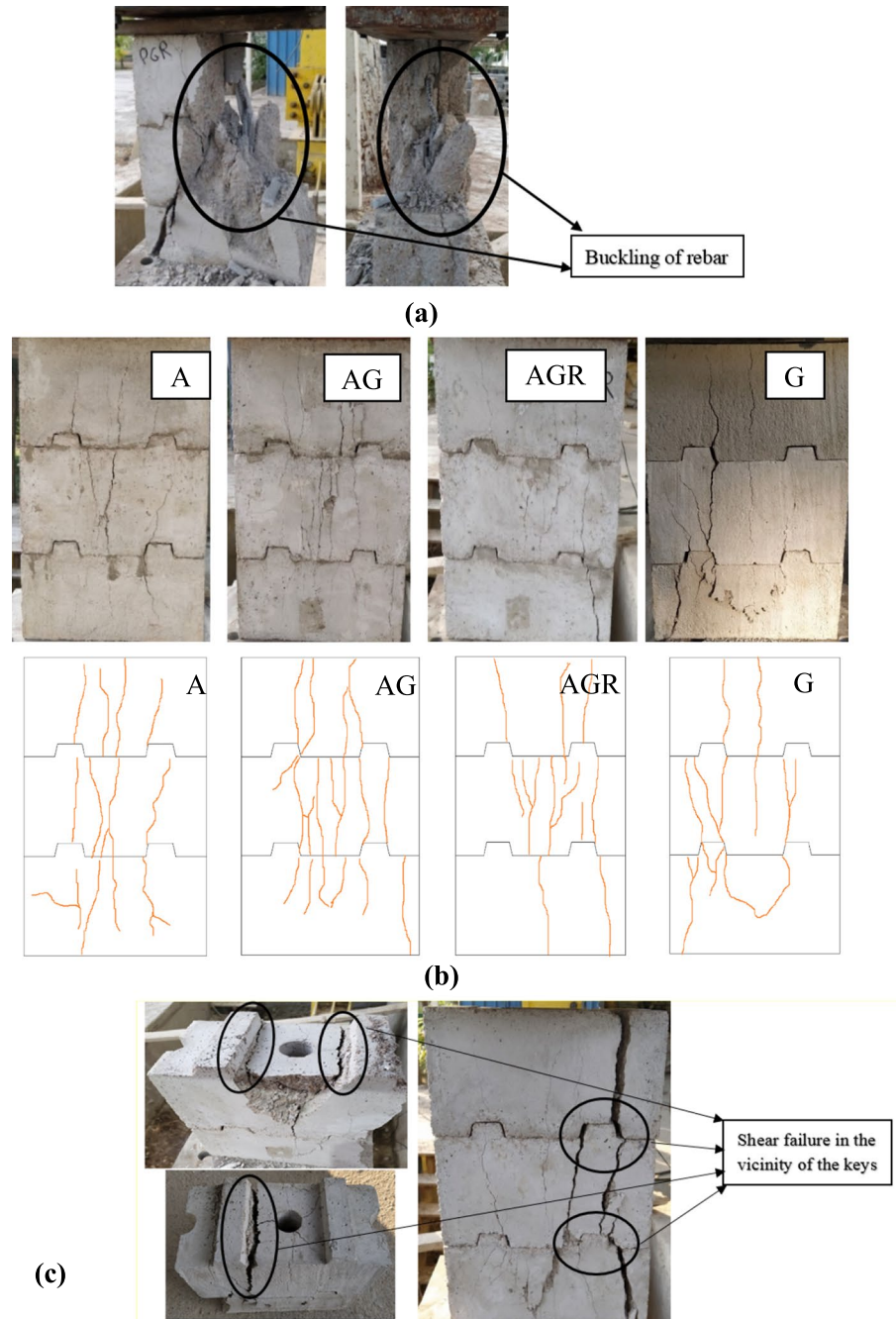**Fig. 6** Stress–strain diagram of masonry prisms under compression test

Fig. 7 The failure of the masonry prisms: **a**. Rebar buckling in the reinforced masonry prisms, **b**. A, AG, AGR, and G modes, **c**. M mode

(a)

(b)

(c)

6.2 Diagonal shear test

6.2.1 Diagonal shear strength

The average of the results of the diagonal shear capacity test as well as the characteristics of the force–displacement behavior of the panel samples in the A, AG, AGR, G and GR modes are summarized in Table 3.

The diagonal shear capacities in the AG and AGR modes were significantly higher than that of the A mode. For example, the diagonal shear capacities in the AG and AGR modes were respectively 151% and 126% more than that of the A mode. As a result, the

Table 3 Properties of masonry panels under diagonal shear test

Panel interconnection type	Diagonal load strength (kN)	Pre-crack secant stiffness (kN/mm)	Displacement at peak load (mm)	Total energy to reach peak load (kN.mm)	Δ_u/Δ_{cr}
A	55.7 (12)	169.2 (15)	0.41 (16)	11.2 (15)	2.1 (12)
AG	140.2 (9.3)	313.8 (12)	0.88 (17)	82.5 (12)	3.1 (11)
AGR	126.3 (10)	406.5 (15)	1.24 (15)	125.3 (11)	6.7 (9.2)
G	30.2 (8.9)	60.5 (12)	2.4 (13)	28.3 (14)	7.2 (11)
GR	81.3 (9.6)	63.3 (19)	1.4 (16)	95.3 (10)	8.1 (13)

Value in parentheses represent coefficient of variation in percentage

use of paste and grout as interconnecting elements is significantly effective in increasing the diagonal shear capacity of the block panels compared to the mode in which only paste or grout is used. This increase in capacity can be due to the considerable contribution of the grout and rebar reinforcement elements in carrying in-plane load. Moreover, the filling of the pasted block holes with grout (AG) had a greater impact on the diagonal shear capacity of the samples compared to the combination of grout and rebar (AGR). This can be mainly attributed to adverse effect of installing rebar on the behavior of grout due to the possible insertion of cavity.

The in-plane shear capacity dropped 46% in the grouted case (G) compared with the pasted case (A). The strength of the GR case was also 35% lower than

that of the AGR case. In G mode, the space between the shear keys of the block was empty, and consequently, the load was mainly supported by the friction between the blocks and the grout. As a result, the diagonal shear capacity of the G mode was lower than that of the other modes.

6.2.2 Force–displacement characteristics

Figure 8 depicts the force-vertical displacement diagram (along compressive diameter). Table 3 presents displacement at the maximum load and pre-cracking secant stiffness of the diagonal panels. By dividing the ultimate displacement by the displacement regarding to cracking point observed in the diagonal panels, a coefficient is defined to introduce relative

Fig. 8 Force–displacement diagram of panels under diagonal shear test
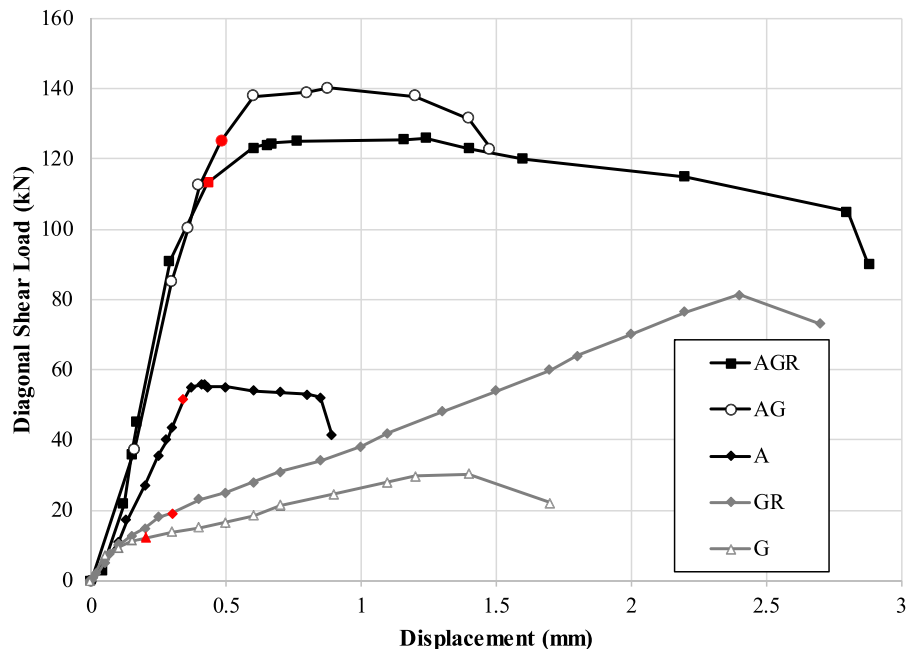
ductility, given as Δ_u/Δ_{cr} in Table 3. The cracking point is highlighted with a solid red point in Fig. 8.

Among the modes with adhesive paste, the AGR and A modes have the highest and lowest displacement at the maximum load, respectively. Moreover, by reinforcing the diagonal panels with grout (AG) and with grout and rebar (AGR), it can be observed that the displacement at the maximum load and the ductility coefficient increase. For instance, reinforcing the pasted panels with grout (AG) and with grout and rebar (AGR) results in a 114 and 202% increase in displacement at the maximum load, respectively. Additionally, the ductility coefficient increases by 49 and 224%, respectively, when compared to the A mode. As a result, adding rebar to grout in pasted panels has a greater effect on displacement and ductility compared to the diagonal shear capacity.

According to Fig. 8 and the displacement values in Table 3, adding rebar to grout in diagonal panels effectively increases the ductility although it causes a slight decrease in the diagonal shear capacity. This could be because parts of the holes in the blocks are left empty when filled with rebar.

In addition to ductility, by adding grout and grout and rebar to the connections of the diagonal panels, the energy dissipation of the panels increases significantly compared to the A mode. Thus, the addition of grout and grout with rebar to the adhesive connection in the diagonal panels has a more significant impact on energy dissipation rather than ductility.

When the holes of the diagonal panels are filled with grout, the AG and AGR modes exhibit a considerably higher initial stiffness in the panels compared to the A mode. This is attributed to the higher compressive strength of the grout and interaction between the blocks in comparison to the pasted mode.

To understand the contribution of adhesive paste to the diagonal shear behavior of panels, two interconnection cases of G and GR were also tested. The stiffness and strength were considerably higher in the pasted cases (A, AG, and AGR) than in the G and GR modes. When paste filled the gap between the shear keys, they were completely engaged in load transfer. In the absence of adhesive paste, the gap between the blocks facilitated the relative movement of the blocks, which resulted in significantly lower strength and stiffness but in a higher peak displacement. The stiffness of G mode was 81% lower compared to AG mode, while the stiffness of

GR mode was 84% lower than that of AGR mode. Therefore, the utilization of adhesive paste demonstrated an enhancement in both the in-plane stiffness and strength, while it had an adverse effect on the ductility. This brittle behavior, however, can be mitigated to a significant extent through the incorporation of rebar (AGR versus AG).

### 6.2.3 Crack and type of failure

By examining the diagonal panels, two types of failure (sudden or brittle and gradual or semi-brittle) were mainly observed. The failures of the panels in the AGR and GR modes were more of the gradual, semi-brittle, and ductile types due to the presence of rebar with grout. The curve in Fig. 8 also confirms the ductility of the panels in the AGR and GR modes. However, the failures of the panels in the A, AG and G modes were quite sudden and brittle so that the samples suddenly failed and were divided into two or more parts after reaching the breaking point.

In the AG, AGR, and GR modes, the panels experienced failure along their diameter in the form of shear failure of the interlocking keys. However, it should be noted that the failure mechanism in the A and G modes primarily involved the opening of the block joints. This can be attributed to the weak adhesion of the connections between the blocks in the G mode and the absence of vertical restraints to prevent block separation in the A mode. Due to this reason, there were substantial differences in the diagonal capacities of the panels in the AG, AGR, and GR modes compared to the A and G modes. Consequently, the keys of the blocks played a crucial role in bearing the in-plane shear force. The failure types of the panels are illustrated in Fig. 9.

In the absence of adhesive paste in modes G and GR, combined with the presence of the gap between the shear keys, there was a possibility of block sliding as the load increased. Thus, in these modes, the engagement of the shear keys happened at an earlier stage compared to the modes with adhesive paste (A, AG, and AGR). As a result, the occurrence of initial cracking in the modes without adhesive paste emerged earlier than in the cases where paste was present. The diagram in Fig. 8 depicts the initial cracking points, which are indicated by the highlighted red points.

Fig. 9 The failure of the diagonal panels
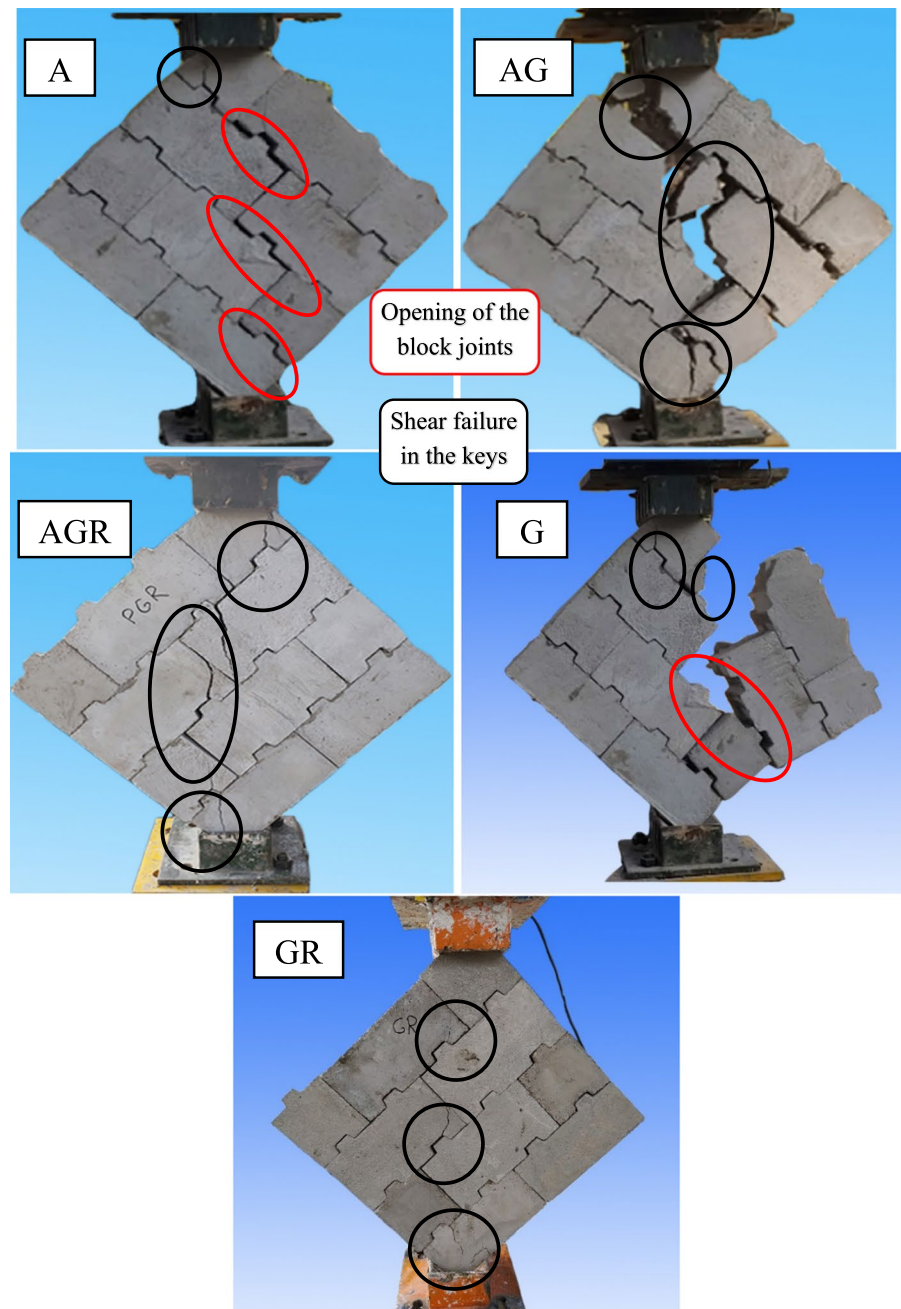
6.3 In-plane shear test

6.3.1 Shear strength

The shear capacity obtained from the in-plane shear test can be seen in Table 4. Although G-type samples were prepared, due to their low strength and brittle behavior, they broke during handling under the self-weight effect and no test results were reported accordingly. The shear behavior is a key factor in the seismic performance of masonry structures. The in-plane shear force of the block samples is supported through the friction between the blocks, the physical engagement of the keys, as well as different interconnection conditions such as adhesive, grout, and rebar.

Table 4 Properties of masonry samples under in-plane shear test

Prism connection type	Shear strength (kN)	Secant stiffness (kN/mm)	Displacement at peak load (mm)	Total energy to reach peak load (kN.mm)
A	37.3 (8.9)	21.6 (12)	2.87 (11)	49.4 (10)
AG	45.3 (7.5)	17.5 (10)	3.08 (12)	67.5 (11)
AGR	75.0 (6.6)	17.0 (13)	3.72 (14)	126.5 (14)
GR	34.3 (9.1)	15.9 (15)	2.90 (13)	41.3 (15)

Value in parentheses represent coefficient of variation in percentage

The shear capacity of the GR mode was lower compared to the other modes. The main reasons are the low shear strength of the grout, the presence of the gap between the keys, and the lack of engagement between the keys. Conversely, in the AGR mode, the filling of the empty space between the keys with paste, combined with the joint shear action of adhesive paste, keys, grout, and rebar, significantly affects the shear capacity. As a result, the shear capacity of the AGR mode was significantly higher than other modes. For instance, by adding grout (the AG mode), the capacity increased by 21% compared to the A mode. Moreover, by adding rebar to the grout (the AGR mode), the shear capacity of the samples increased around 66% compared to the AG mode.

As a result, the addition of reinforcing bars in the grout demonstrated a greater enhancement in the shear capacity of the samples during the triplet test, compared to filling the holes with grout alone. This improvement can be attributed to the positive shear performance provided by the bars embedded within the grout. This finding is consistent with the results reported in Ma's research [35].

The shear strength of the GR case was slightly (8%) less than that of the pasted samples (A). It should be noted that the shear strength of the AGR mode was almost equal to the sum of A and GR capacities. This shows that the shear strength of each interconnection condition can be added directly to find the total shear capacity. In this regard, the low shear strength of the G-case could be predicted from the small difference between the A and AG modes.

6.3.2 Force–displacement characteristics

The force–displacement relationship of the shear samples in the in-plane shear test is plotted in Fig. 10 and displacement at the maximum load, secant stiffness and energy dissipation are also presented in Table 4. The initial slopes of the force–displacement curve (initial stiffness) in pasted modes (A, AG, and AGR) are almost equal up to the displacement range of 0.5 mm. This can be due to the joint action of the adhesive and inter-block friction in this displacement range. In other words, in this displacement range, the adhesive and friction at first play a resisting role against shear force. Then, after the loss of adhesive resistance, other interconnection elements such as block shear keys, grout, and rebar resist against shear force. In Fig. 10, this can be interpreted from the displacement of about 0.5 mm in all cases. The influence of inter-block friction has also been mentioned in previous studies [50].

After the displacement range of 0.5 mm when the adhesive bond failed, in the A mode, the block keys and friction, in the AG mode, the keys together with grout and friction, and in the AGR mode, the keys, grout, friction, and rebar play a resisting role against the shear force. For this reason, after this range, the AGR mode has the highest stiffness and the A mode has the lowest stiffness. Adding rebar to grout and adhesive (the AGR mode) has a greater effect on displacement at the maximum load of shear samples than adding grout to adhesive (the AG mode). For example, displacement at the maximum load in the AG mode is 7% more than that of the A mode, whereas this amount of displacement in the AGR mode is 20% more than that of the AG mode. Comparing the peak displacements of the A and GR modes reveals that the failure of the grout and the adhesive bond occurred simultaneously. Among the different modes tested, the GR mode has the lowest initial stiffness. This can be attributed to the absence of paste in this mode. A similar trend of results was also observed in the diagonal test.

The samples in the A and AGR modes respectively have the lowest and highest amount of energy dissipation to reach the maximum load. In addition, the presence of rebar in the grout (the AGR mode) causes a significant increase in the amount of energy

Fig. 10 Force–displacement diagram of triplet samples under in-plane shear test
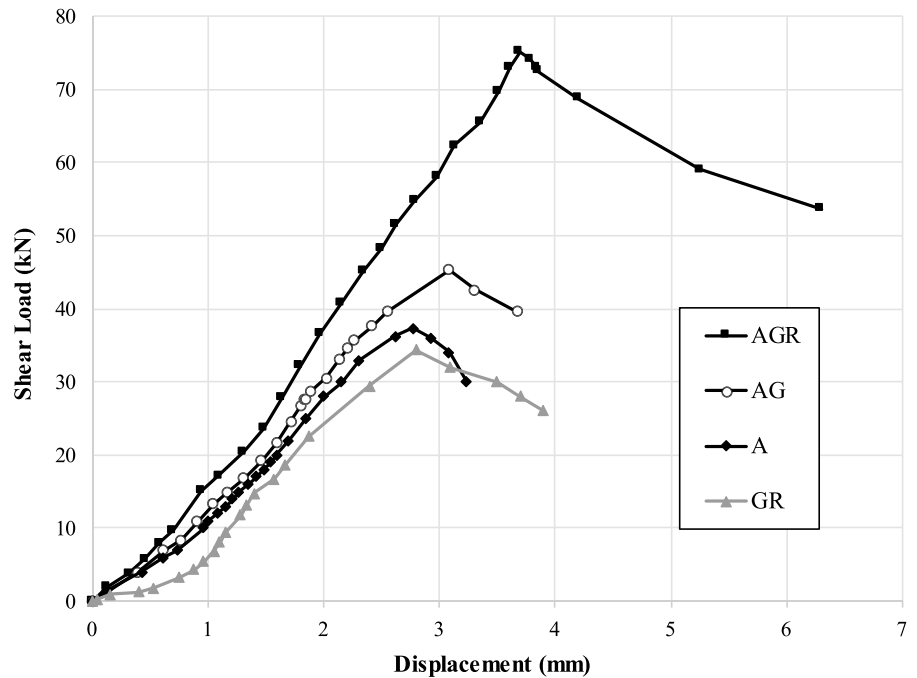
dissipation compared to the presence of grout in the holes (the AG mode) and the use of adhesive alone (the A mode). For instance, the amount of energy dissipation of the AG mode is 36% more than that of the A mode. As a result, adding grout and rebar in the shear samples has a greater effect on the energy dissipation compared to the peak load displacement.

6.3.3 Crack and type of failure

By investigating the type of failure of the shear samples in different modes, it can be concluded that after the keys are locked together and with a gradual increase of force, a shear type of failure was observed in the keys of the blocks in all connection modes. This means that the designed keys of the proposed blocks played an effective role in bearing the in-plane shear force. Figure 11 shows the shear failure of the block keys in the in-plane shear test.

As can be seen in Fig. 11, in addition to the shear failure of the keys, the grout also suffered a brittle shear failure in the AG mode. Moreover, in the A and AG modes, the samples were separated immediately after the sudden failure. However, in the AGR and GR modes, due to the presence of the rebar, the samples experienced a gradual failure and all the reinforcing elements (key, grout, and rebar) resisted against the

shear force. This can be the reason for the increase in the shear capacity and non-fragile response of the AGR mode compared to the other two pasted modes. The sample connected only by grout (G) had a brittle behavior and a very low strength. Thus, the application of grout alone is not proper for in-plane loads such as the seismic effect.

6.4 Comparison of interlocking blocks with conventional masonry

Conventional masonry specimens, consisting of solid or hollow clay bricks and 3:1 sand-cement mortar, were studied by the authors [41, 51]. The compressive strength of the solid brick, hollow brick, and mortar was found to be 13.3 MPa, 11.1 MPa, and 20.4 MPa, respectively. In the present study, the AG condition of the interlocking block demonstrated favorable results in terms of in-plane behavior. Compared to the highest results of the conventional masonry specimens, the AG interlocking block showed an increase of 112% in compressive strength, 31% in diagonal tension strength, and 78% in in-plane shear strength. For the pasted interlocking system (A) without a vertical joint between the blocks, the relative change of compression, diagonal tension, and in-plane shear strengths are 86, −49, and 46%, respectively. These

Fig. 11 The failure of the shear samples
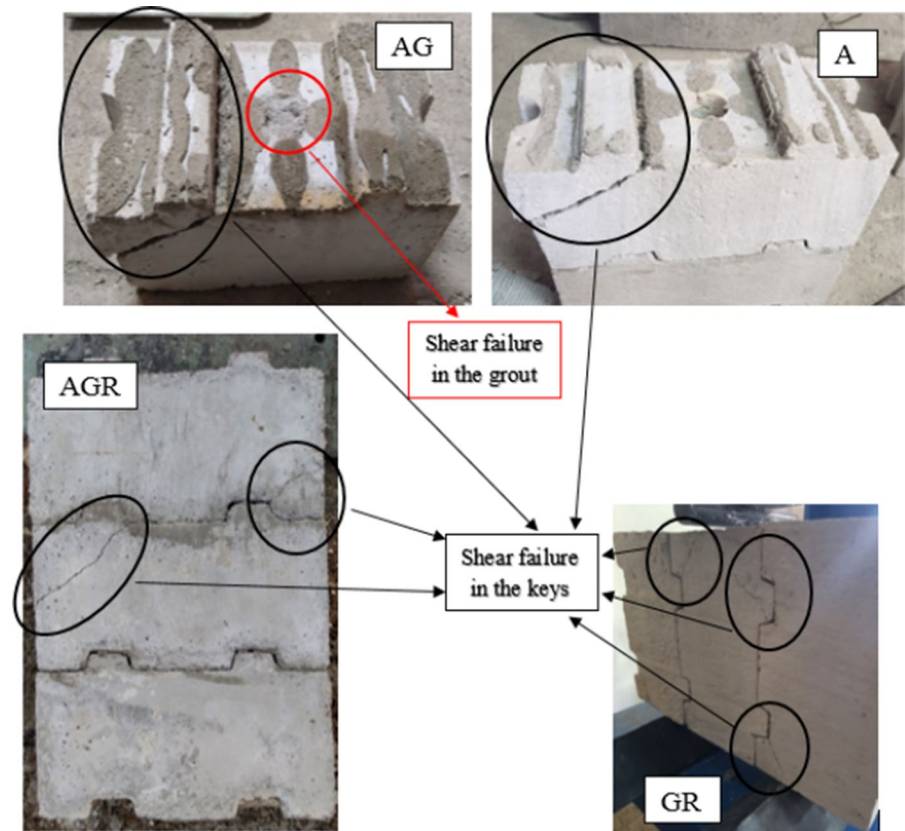
results demonstrate the considerable advantage of the interlocking block system and underscore the crucial role of grouting in the intercking system as the vertical interconnection mechanism.

7 Conclusion

In this experimental study, the in-plane behavior of the samples constructed with the proposed interlocking block was studied in different interconnection conditions (A, AG, AGR, G, and GR). The results showed that the keys and holes designed in the interlocking system had an effective role in enhancing the in-plane behavior of the fabricated samples. By comparing and summarizing the results of the compression, diagonal tension, and in-plane shear tests, the following conclusions were obtained:

- Under compression loading, the addition of grout to the interconnection of the block prisms had the most beneficial effect on improving the strength

among different connection conditions. Adding adhesive paste, grout, and rebar (the AGR mode) to the mortarless prisms significantly enhanced the compressive capacity and slightly improved the stiffness.

- Instead of using a combination of grout and rebar, the utilization of grout in the pasted diagonal panels (AG vs. AGR) led to a higher diagonal tensile strength of the pasted panels (A). On the other hand, adding the steel rebar (AGR) considerably enhanced the energy dissipation capacity and ductility of the panels. In comparison to using adhesive alone, the incorporation of grout or grout combined with rebar in the panel specimens altered the failure mode observed during the diagonal test. Instead of witnessing the opening of the block joints, the panels exhibited a shift towards shear failure of the interlocking keys.

- In the in-plane shear test, the triplet specimens with adhesive paste (A, AG, and AGR modes) had shear key failure since the keys were properly locked together. Accordingly, the presence of rebar (AGR

and GR) had a substantial positive influence on the shear strength, energy dissipation, and ductility.

- In the tests where the loading directly engages the keys, such as diagonal and direct shear tests, the presence of adhesive paste considerably increases the capacity and initial stiffness. However, it may reduce the ductility to some extent.
- In the tested samples, the adhesive paste alone (A) exhibited favorable performance in terms of strength and non-brittle behavior, particularly under compression loads, when compared to the other cases examined.
- The addition of grout to the adhesive paste (AG) had a positive impact on capacity in the diagonal shear, in-plane shear, and compression tests, respectively. Furthermore, it also showed a favorable effect on ductility in the diagonal shear, compression, and in-plane shear tests, respectively.
- The utilization of adhesive paste, grout, and rebar in combination (AGR) led to a significant increase in strength in both in-plane shear and compression tests. Furthermore, this addition demonstrated notable enhancement in terms of ductility in both diagonal shear and in-plane shear tests.

In summary, the addition of adhesive paste and grout (AG) to the interlocking block would significantly enhance the in-plane strength of the interlocking block system. However, to mitigate brittle behavior and to achieve some level of ductility under extreme events such as earthquakes the combination of grout, rebar, and adhesive paste (AGR) to the interlocking system is necessary.

Data availability Data will be made available on request.

Declarations

Conflict of interest The authors declared no potential conflicts of interest with respect to the research, authorship, and/or publication of this article.

References

1. Shi T, Zhang X, Hao H, Chen C (2021) Experimental and numerical investigation on the compressive properties of interlocking blocks. Eng Struct 1(228):111561. https://doi.org/10.1016/j.engstruct.2020.111561
2. Qu B, Stirling BJ, Jansen DC, Bland DW, Laursen PT (2015) Testing of flexure-dominated interlocking compressed earth block walls. Constr Build Mater 15(83):34–43. https://doi.org/10.1016/j.conbuildmat.2015.02.080
3. Murray EB (2007) Dry stacked surface bonded masonry: Structural testing and evaluation. Brigham Young University.
4. Uzoegbo HC, Senthivel R, Ngowi JV (2007) Loading capacity of dry-stack masonry walls. Masonry Soc J 25(1):41–52
5. Casapulla C, Mousavian E, Zarghani M (2019) A digital tool to design structurally feasible semi-circular masonry arches composed of interlocking blocks. Comput Struct 1(221):111–126. https://doi.org/10.1016/j.compstruc.2019.05.001
6. Dyskin AV, Pasternak E, Estrin Y (2012) Mortarless structures based on topological interlocking. Front Struct Civ Eng 6:188–197. https://doi.org/10.1007/s11709-012-0156-8
7. Martínez M, Atamturktur S (2019) Experimental and numerical evaluation of reinforced dry-stacked concrete masonry walls. J Build Eng 1(22):181–191. https://doi.org/10.1016/j.jobe.2018.12.007
8. Anand KB, Ramamurthy K (2003) Laboratory-based productivity study on alternative masonry systems. J Constr Eng Manage 129(3):237–242. https://doi.org/10.1061/(ASCE)0733-9364(2003)129:3(237)
9. Liu H, Liu P, Lin K, Zhao S (2016) Cyclic behavior of mortarless brick joints with different interlocking shapes. Materials 4;9(3):166. https://doi.org/10.3390/ma9030166
10. Sturm T, Ramos LF, Lourenço PB (2015) Characterization of dry-stack interlocking compressed earth blocks. Mater struct 48:3059–3074. https://doi.org/10.1617/s11527-014-0379-3
11. Thanoon WA, Jaafar MS, Kadir MR, Ali AA, Trikha DN, Najm AM (2004) Development of an innovative interlocking load bearing hollow block system in Malaysia. Constr Build Mater 18(6):445–54. https://doi.org/10.1016/j.conbuildmat.2004.03.013
12. Bragança L, Pinheiro M (2010) Portugal SB10: sustainable building affordable to all: low cost sustainable solutions. Universidade do Minho
13. Edwards J, Gayed M, Pyra M, Rodriguez T (2010) Design and Construction of Interlocking Mortarless Block Masonry. In2nd masonry mini symposion Edmonton alberta
14. Gallegos H (1988) Mortarless masonry: the Mecano system. Int J Housing Sci Appl 12(2):145–157
15. Drysdale RG, Gazzola E (1991) Strength and deformation properties of a grouted, drystacked, interlocking, concrete block system. Brick and block masonry, pp164–71
16. Drysdale RG, Eng P (2005) Properties of Azar dry-stack block-IV construction. Hamilton, Ontario, p 758.
17. Anand KB, Ramamurthy K (2005) Development and evaluation of hollow concrete interlocking block masonry system. Masonry Soc J 23(1):11–19
18. Al-Fakih A, Mohammed BS, Liew MS (2018) Behavior of the dry bed joint in the mortarless interlocking masonry system: an overview. Civ Eng Res J 4(5)

19. Maïni S (2005) Earthen architecture for sustainable habitat and compressed stabilised earth block technology. The Auroville Earth Institute. Auroville Building Center-India 14(4):112–28.

20. Uzoegbo HC, Ngowi JV (2003) Structural behaviour of dry-stack interlocking block walling systems subject to in-plane loading. Concr Beton 103:9–13

21. Haener, (1984) Stacking mortarless block system. Engineering Design Manual by Ikinson Engineering Inc, Hamilton, Ontario

22. Jeslin AJ, Padmanaban I (2020) Experimental studies on interlocking block as wall panels. Mater Today Proc 1(21):1–6. https://doi.org/10.1016/j.matpr.2019.05.294

23. Qamar F, Thomas T, Ali M (2020) Improvement in lateral resistance of mortar-free interlocking wall with plaster having natural fibres. Constr Build Mater 234:117387. https://doi.org/10.1016/j.conbuildmat.2019.117387

24. Baneshi V, Dehghan SM (2021) Introducing a novel interlocking block and experimental study on in-plane and out-of-plane behavior and strength of its prisms specimens. J Struct Construct Eng 334–354 (in Persian) https://doi.org/10.22065/JSCE.2021.246795.2226

25. Ngapeya GG, Waldmann D (2020) Experimental and analytical analysis of the load-bearing capacity Pu of improved dry-stacked masonry. J Build Eng 1(27):100927. https://doi.org/10.1016/j.jobe.2019.100927

26. Glitza H (1991) State of Art and Tendency of Development of Masonry without Mortar. Brick and Block Masonry 2:1028–1033

27. Lohr JR (1992) Evaluation of "Formwall": a post-tensioned dry-stacked masonry system. MS. thesis, The Pennsylvania State University

28. Marzahn G (1997) Dry-stacked masonry in comparison with mortar jointed masonry. Leipzig Ann Civil Eng Rep 2:353–365

29. Biggs DT (2002) Development of a mortarless post-tensioned masonry wall system. In: Proceedings of the sixth international masonry conference, pp 28–32

30. Biggs DT, Forsberg TE (2008) A mortarless prestressed masonry house: case study. Proceedings of the 14th international brick and block masonry conference, Australia, pp 1–11

31. Sokairge H, Rashad A, Elshafie H (2017) Behavior of post-tensioned dry-stack interlocking masonry walls under out of plane loading. Constr Build Mater 133:348–357. https://doi.org/10.1016/j.conbuildmat.2016.12.071

32. Xie G, Zhang X, Hao H, Bi K, Lin Y (2022) Response of reinforced mortar-less interlocking brick wall under seismic loading. Bull Earthquake Eng 20(11):6129–6165. https://doi.org/10.1007/s10518-022-01436-6

33. Kasinikota P, Tripura DD (2022) Flexural behavior of hollow interlocking compressed stabilized earth-block masonry walls under out-of-plane loading. J Build Eng 1(57):104895. https://doi.org/10.1016/j.jobe.2022.104895

34. Kohail M, Elshafie H, Rashad A, Okail H (2019) Behavior of post-tensioned dry-stack interlocking masonry shear walls under cyclic in-plane loading. Constr Build Mater 30(196):539–554. https://doi.org/10.1016/j.conbuildmat.2018.11.149

35. Ma H, Ma Q, Gaire P (2020) Development and mechanical evaluation of a new interlocking earth masonry block.

36. Zahra T, Dorji J, Thamboo J, Asad M, Kasinski W, Nardone A (2023) In-plane and out-of-plane shear characteristics of reinforced mortarless concrete block masonry. J Build Eng 1(66):105938. https://doi.org/10.1016/j.jobe.2023.105938

37. Baneshi V, Dehghan SM, Hassanli R (2023) An experimental study on the behavior of interlocking masonry blocks manufactured using 3D printed mold. Adv Struct Eng 26(2):360–380. https://doi.org/10.1177/13694332221126595

38. Ayed HB, Limam O, Aidi M, Jelidi A (2016) Experimental and numerical study of interlocking stabilized earth blocks mechanical behavior. J Build Eng 1(7):207–216. https://doi.org/10.1016/j.jobe.2016.06.012

39. Casapulla C, Mousavian E, Argiento L, Ceraldi C, Bagi K (2021) Torsion-shear behaviour at the interfaces of rigid interlocking blocks in masonry assemblages: experimental investigation and analytical approaches. Mater struct 54(3):134. https://doi.org/10.1617/s11527-021-01721-x

40. Casapulla C, Argiento LU, Maione A, Speranza E (2021) Upgraded formulations for the onset of local mechanisms in multi-storey masonry buildings using limit analysis. Structures 31:380–394. https://doi.org/10.1016/j.istruc.2020.11.083

41. Dehghan SM, Najafgholipour MA, Baneshi V, Rowshanzamir M (2018) Mechanical and bond properties of solid clay brick masonry with different sand grading. Constr Build Mater 20(174):1. https://doi.org/10.1016/j.conbuildmat.2018.04.042

42. Dehghan SM, Najafgholipour M, Baneshi V, Rowshanzamir M (2019) Experimental study on effect of water-cement ratio and sand grading on workability and mechanical properties of masonry mortars in Iran. Iran J Sci Technol Trans Civ Eng 43:21–32. https://doi.org/10.1007/s40996-018-0110-7

43. ASTM C109–07 (2007) Standard test method for compressive strength of hydraulic cement mortars. American Society for Testing and Materials International, Philadelphia

44. ASTM C348 (1997) Test method for flexural strength of hydraulic mortar. American Society for Testing and Materials International, Philadelphia

45. ASTM C1437 (2007) Standard test method for flow of hydraulic cement mortar. American Society for Testing and Materials International, Philadelphia

46. ASTM C1107 (2011) Standard specification for packaged dry, hydraulic-cement grout (Nonshrink). American Society for Testing and Materials International, Philadelphia

47. ASTM C1314 (2010) Standard test method for compressive strength of masonry prisms. American Society for Testing and Materials International, Philadelphia

48. ASTM E519 (2012) Standard test method for diagonal tension (shear) in masonry assemblages. American Society for Testing and Materials International, Philadelphia

49. Rilem MS (1996) Determination of shear strength index for masonry unit/mortar junction. Mater Struct 29:459–475

50. Tang Z, Ali M, Chouw N (2014) Residual compressive and shear strengths of novel coconut-fibre-reinforced-concrete

Adv Struct Eng 23(2):234–247. https://doi.org/10.1177/1369433219868931

interlocking blocks. Constr Build Mater 15(66):533–540. https://doi.org/10.1016/j.conbuildmat.2014.05.094

51. Dehghan SM, Baneshi V, Yousefi Kahnooj S, Najafgholi-puor MA (2022) Experimental study on effect of brick and mortar types on mechanical properties of masonry prisms. J Struct Construct Eng 8(11):5–24 (**(in Persian)**)https://doi.org/10.22065/JSCE.2021.252499.2259

Publisher's Note Springer Nature remains neutral with regard to jurisdictional claims in published maps and institutional affiliations.